A Robust Autonomous Vehicular Navigation System Using RIMU-based INS/GNSS Integrated Scheme

Kai-Wei Chiang[1] , Chi-Hsin Huang [1]* , Yu-Ting Chiu[2] , Ting-Chun Wu[3], Syun Tsai [3], Kuan-Ying Lin[3]
[1] Department of Geomatics, National Cheng Kung University, Taiwan – (kwchiang, windstorm) @geomatics.ncku.edu.tw
[2] Department of Geomatics, National Cheng Kung University, Taiwan – (p66081106) @gs.ncku.edu.tw
[3] Department of Geomatics, National Cheng Kung University, Taiwan – (easy3123, dino920135, azsxd2014) @gmail.com

KEYWORDS: Inertial Navigation System (INS), Global Navigation Satellite Systems (GNSS), Redundant Inertial Measurement Unit (RIMU), Micro Electro Mechanical Systems (MEMS)

ABSTRACT:

The application of the INS/GNSS integrated system is widespread in vehicle navigation. However, in certain complex urban areas, achieving accurate positioning for autonomous vehicles at level 3 and beyond presents a challenge. Moreover, ensuring the continuous availability of the navigation system is crucial for maintaining vehicle safety under all circumstances. Consequently, the specifications of the Inertial Measurement Unit (IMU), which have a direct correlation with cost, dominate the performance of the navigation system in environments where GNSS signals are denied or challenging. To implement level 3 autonomous vehicles, a strategy based on redundant IMUs (RIMU) is employed to not only enhance accuracy and availability but reduce the overall cost of the navigation system. This research mainly focuses on the development of a robust autonomous vehicular navigation system by designing an integrated algorithm for the low-cost RIMU and GNSS receiver within the INS/GNSS integration scheme. The positioning performance is analyzed by using a reference system and a benchmark system in the open sky, GNSS challenging, and GNSS outage scenarios.

1. INTRODUCTION

The Society of Automotive Engineers (SAE, 2018) has established a six-level framework for road vehicle autonomy, with level 3 (conditional automation) being crucial in autonomous vehicle development. Beyond level 3, the system has to monitor and perform dynamic driving tasks (Reid et al., 2019). This study focuses on developing the navigation system of level 3 autonomous vehicles and evaluating their performance in challenging scenarios. Accurate positioning at the "Which Lane" (1.5 meters) or "Where in Lane" (0.5 meters) level is essential for achieving necessary accuracy in level 3 and higher autonomous vehicles, as defined by Alves et al. (2010) and Stephenson et al. (2016).

The integration of the Global Navigation Satellite System (GNSS) and Inertial Navigation System (INS) is commonly used in vehicle navigation applications. In open sky scenarios, the INS/GNSS integrated system can meet the “Which Lane” level criteria with a reliable GNSS solution. Moreover, the "Where in Lane" level can be reached with Real-Time Kinematic (RTK) services. However, GNSS faces challenges in scenarios such as urban canyons, underpasses, tunnels, and indoor environments, where signal availability decreases due to signal obstruction, Multipath Interference, and Non-line-of-sight (NLOS) Reception. In prolonged GNSS-denied environments, the drift of the INS becomes dominant, and the quality of the Inertial Measurement Unit (IMU) plays a critical role in maintaining high positioning accuracy.

Therefore, tactical-grade IMUs such as EPSON G320 and EPSON G370 are required for highly accurate positioning, but their high cost makes them unsuitable for the commercialization and industrialization of level 3 autonomous vehicles. Therefore, a strategy based on redundant IMUs (RIMU) is proposed to improve the positioning accuracy and enhance the availability of the conventional INS/GNSS integrated system by using Micro Electromechanical Systems (MEMS) consumer-grade IMU. This research makes the following contributions:

1. A Robust Autonomous Vehicular Navigation System is developed by using the low-cost RIMU and GNSS receiver and INS/GNSS integrated algorithm.
2. The long-term GNSS outage scenario (around 5 minutes) is tested to analyze the improvement of the RIMU (Triple redundant) compared to a single IMU (SIMU).
3. In addition to the GNSS outage scenario, the GNSS challenging scenarios and open sky scenarios are also tested to evaluate the availability and the environmental adaptability of the proposed system.
4. A trustable reference system is applied to analyze the accuracy of the developed testing system which can be compared to a benchmark system (NovAtel PwrPak7D-E2).

2. METHODOLOGY

A conventional INS/GNSS integrated system, which uses the Extended Kalman Filter (EKF) is applied in this research (Figure 1). In the navigation filter, the INS was chosen as the primary system; nevertheless, it encountered challenges related to the accumulation of errors arising from bias and scale factor drift. To address this issue, the integration of INS, GNSS, and some virtual measurements, i.e., motion constraints is employed, specifically adopting the loosely coupled (LC) integration scheme in this research. Since the navigation solutions of INS and GNSS are estimated independently by two separate estimators, a solution backup exists (El-Sheimy, 2006). This design is suitable for a robust autonomous vehicular navigation system, which has to provide continuous availability of solutions all the time.

Moreover, this architecture is easy to implement and extend due to consistent and fewer navigation states. This LC integration scheme can be modularized to activate or deactivate any measurement. In fact, the solutions of an independent Visual-Inertial Navigation System (VINS) are added as measurement updates in our other advanced research. On the other hand, the raw measurements of RIMU are fused before being inputted into the EKF, that is, the solutions of INS are estimated through a virtual IMU. This processing also follows the concept of LC.

* Corresponding author

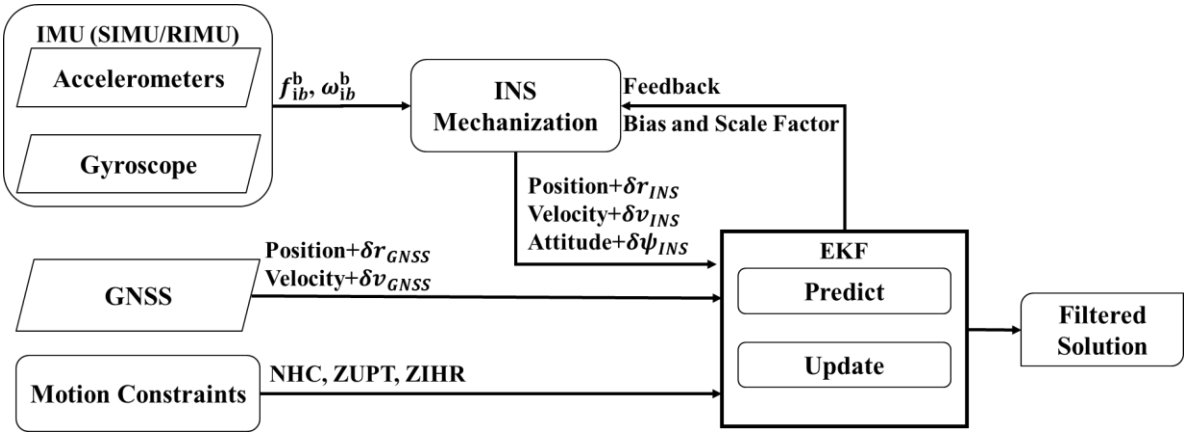

Figure 1. The flowchart of loosely coupled INS/GNSS integration scheme

2.1 Motion Constraints

In addition to the GNSS measurement (position and velocity), the motion constraints such as Non-holonomic constraints (NHC), Zero Velocity Update (ZUPT), and Zero integrated heading rate (ZIHR), which using virtual measurements are adopted to improve the navigation solution. The ZUPT and the ZIHR, utilize the static motion of land vehicles to constrain the velocity error, heading error, and their contribution to the attitude and position error. The utilized virtual measurements rely on the premise that the velocity in every direction on the navigation frame ought to be zero, and the vehicle's heading angle should remain constant. On the other hand, the NHC is employed to control the lateral and vertical velocities, which are considered to be zero when the vehicle is moving longitudinally, in accordance with the typical motion observed in land vehicles. By adopting these kinds of motion constraints, navigation errors can be reduced dramatically. The performance of the INS/GNSS integrated system which uses low-cost MEMS IMU can be improved significantly, especially during the GNSS outage.

2.2 Redundant-IMUs (RIMU)

The RIMU is seen as a virtual IMU, which is used to replace SIMU in the proposed integrated scheme. This RIMU is constructed by triple IMUs, which have the same specifications as SIMU. The improvement of RIMU in the INS/GNSS integrated system is evaluated in comparison with SIMU under the same conditions.

2.2.1 Error Propagation

The fundamental RIMU theory is based on error propagation. By averaging the observations of N IMUs (X_i) with the same specifications and axial direction, the noise (σ) can be reduced by a factor of $1/\sqrt{N}$, leading to a substantial decrease in several error terms especially the gyro bias instability (BI). This specific error propagation is described in Equation (1) and Equation (2).

$$\because \bar{X} = \frac{\sum_{i=1}^{N} X_i}{N}, \sigma_{X_i} = \sigma \quad (1)$$

$$\therefore \sigma_{\bar{X}} = \sqrt{\sum_{i=1}^{N} \frac{\sigma_{X_i}^2}{N^2}} = \sqrt{N \cdot \frac{\sigma^2}{N^2}} = \frac{\sigma}{\sqrt{N}} \quad (2)$$

On the other hand, the IMUs with different specifications or mounted misaligned still can be implemented, but the error propagation becomes nonlinear and more complicated. Additionally, the configuration of RIMU, including optimal geometry, systematic error reduction, and lever arm effect, has been extensively discussed in previous studies (Waegli et al., 2008; Jafari, 2015; Martin et al., 2013; Cho et al., 2021). The design matrix derived from the configuration of RIMU can be used to estimate the error through the covariance matrix and determine the optimal geometry according to geometric dilution of precision (GDOP). However, our research focuses mainly on the noise reduction effectiveness mentioned above. The lever arm is designed for negligible, and the axes of sensors are aligned. This kind of RIMU is attributed to the utilization of MEMS technology, which reduces the volume, power consumption, and cost of IMU. Therefore, multiple IMUs can be integrated into a single Printed Circuit Board (PCB).

2.2.2 Fusion Algorithms

Bancroft and Lachapelle (2011) discuss the adoption of various fusion algorithms for incorporating RIMU in INS/GNSS integration. These fusion algorithms can be classified into three distinct strategies. The first strategy involves projecting the raw measurements from each individual IMU onto a common frame, thereby creating a single virtual IMU. Subsequently, the measurements are fused and can be utilized in the INS/GNSS EKF as shown in Figure 2. The transformation between virtual IMU and individual IMU can be described as Equation (3) and Equation (4):

$$\omega_{in}^{n} = R_{v}^{n} \omega_{iv}^{v} \quad (3)$$

$$f_{in}^{n} = R_{v}^{n} f_{iv}^{v} + R_{v}^{n}(\alpha_{iv}^{v} \times r_{nv}^{v}) + R_{v}^{n}(\omega_{iv}^{v} \times (\omega_{iv}^{v} \times r_{nv}^{v})) \quad (4)$$

where ω_{in}^{n} and ω_{iv}^{v} are the angular velocity of the n^{th} IMU and the virtual IMU respectively, R_{v}^{n} is the rotation matrix from the body frame of the virtual IMU to the n^{th} IMU, f_{in}^{n} and f_{iv}^{v} are the specific force of the n^{th} IMU and the virtual IMU respectively, α_{iv}^{v} is the angular acceleration of the virtual IMU, and r_{nv}^{v} is the lever arm of n^{th} IMU to the virtual IMU.

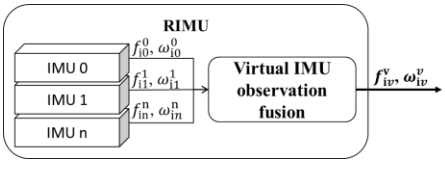

Figure 2. The flowchart of the virtual IMU observation fusion algorithm

In contrast, the centralized filter and federated filter architectures employ the measurements from individual IMUs separately. In other words, all measurements are incorporated into the INS/GNSS EKF. The key distinction between these two architectures lies in the use of either a single stacked filter or multiple parallel filters for processing the INS/GNSS integration.

As stated above, the first virtual IMU observation fusion algorithm is adopted to process the raw measurements in this research because it is easier to be implemented and compared with SIMU without changing the mentioned loosely coupled INS/GNSS integration scheme.

2.2.3 Allan Variance

The Allan Variance is a time-domain analysis method, which can be used to characterize various kinds of noise terms in IMU data. The Allan Variance expresses the root mean square (RMS) random-drift errors as a function of averaging times, which is easy to be implemented and interpreted. (El-Sheimy et al., 2008) The analysis of the Allan variance is instrumental in assessing the bias instability and random walk, both of which hold significant importance in INS. Consequently, these types of noise characteristics often serve as key indicators in IMU specifications and can be utilized for error modeling in EKF.

Figure 3 and Figure 4 depict the corresponding Allan Deviation curves of SIMU and RIMU obtained from gyroscope and accelerometer measurements, respectively. For this analysis, long-term measurements spanning over a duration of more than 10 hours were employed, comprising raw data from the SIMU and fused data from the RIMU. The estimated results are compared to the official specifications as demonstrated in Table 1 and Table 2. The results demonstrate a notable reduction in bias instability from SIMU to RIMU, amounting to approximately $1/\sqrt{3}$ times the original value. Despite the discrepancy between the estimated specifications and the official specifications, which could be attributed to nonideal temperature control, the test results provide corroborating evidence for the fundamental theory discussed earlier. The reduction of bias instability as well as other associated noise terms can be expected to cause a large improvement in replacing the SIMU with RIMU in the proposed LC INS/GNSS integrated system.

The research from De Alteriis et al. (2021) provides similar results from the comparison of Allan Deviation curves of SIMU and RIMU. Moreover, they investigate the performance improvement achieved by integrating consumer-grade MEMS RIMU (Sextuple redundant) into land vehicles using INS/GNSS integration algorithms. Their analysis indicates that the RIMU is competitive with a tactical-grade IMU. In comparison to their research, the long-term GNSS outage (around 5 minutes), GNSS challenging, and open sky scenarios are tested in this research to evaluate the improvement of INS drift, accuracy, and robustness comprehensively. Moreover, a reliable reference system using a navigation grade IMU is adopted to analyze the performance of the navigation solution.

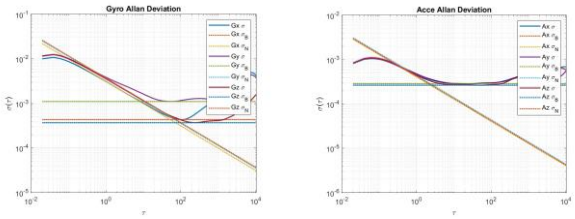

Figure 3. The Allan Deviation curve of SIMU

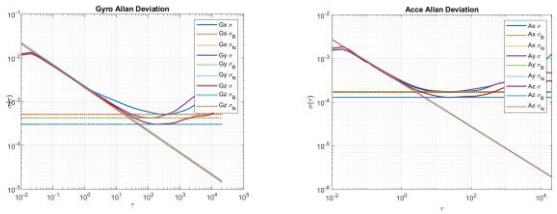

Figure 4. The Allan Deviation curve of RIMU

Table 1. The specifications of SIMU

Official specifications				Test result			
Acc BI (mg)	VRW (m/s/$\sqrt{hr}$)	Gyro BI ($°/hr$)	ARW ($°/\sqrt{hr}$)	Acc BI (mg)	VRW (m/s/$\sqrt{hr}$)	Gyro BI ($°/hr$)	ARW ($°/\sqrt{hr}$)
0.040	0.03	3.0	0.21	0.045	0.03	3.6	0.21

Table 2. The specifications of RIMU

Official specifications				Test result			
Acc BI (mg)	VRW (m/s/$\sqrt{hr}$)	Gyro BI ($°/hr$)	ARW ($°/\sqrt{hr}$)	Acc BI (mg)	VRW (m/s/$\sqrt{hr}$)	Gyro BI ($°/hr$)	ARW ($°/\sqrt{hr}$)
0.015	0.02	1.3	0.08	0.024	0.02	2.2	0.13

3. EXPERIMENT

3.1 Configuration Description

The experimental configuration, illustrated in Figure 5, encompasses three distinct systems: a reference system (iNAV-RQH-1008) equipped with a navigation-grade IMU, a benchmark system (PwrPak7D-E2) comprising a tactical-grade IMU (EPSON G370) and a GNSS receiver (NovAtel OEM7), and the testing systems (RIMU and SIMU), all of which are mounted on the land vehicle. The Inertial Explorer (IE) which is a commercial INS/GNSS software is used to generate a reliable reference trajectory in post-processing by using the IMU data of iNAV-RQH and the GNSS data of NovAtel OEM7. For evaluating the proposed system, the real-time solution provided by the benchmark system is utilized, while the testing solutions

are estimated using the aforementioned loosely coupled algorithm. For the testing system, the low-cost GNSS receiver (Ublox ZED-F9P) is used and constructed with SIMU and RIMU. To ensure consistency, the NovAtel GPS-703-GGG antenna is used and tapped to each system. Furthermore, Table 3 presents a comprehensive comparison of the INS/GNSS navigation system's specifications and costs, effectively highlighting the cost-effectiveness of the proposed system based on RIMU. In addition, all GNSS solutions are estimated using the (RTK) mode in order to maximize the achieved accuracy.,

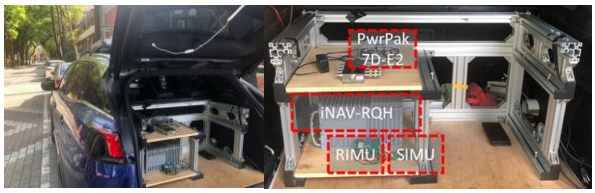

Figure 5. The Configuration of the experimental sensors

Table 3. The specification and the cost of the INS/GNSS navigation system

System	Reference	Benchmark	Testing
IMU	iMAR iNAV-RQH-1008	PwrPak7D-E2 (EPSON G370)	RIMU
Gyro Bias Stability	<0.005 deg/hr	<0.8 deg/hr	~2 deg/hr
Accel. Bias Stability	<0.01 mg	<0.01mg	~0.02 mg
GNSS	NovAtel OEM6	NovAtel OEM7	Ublox ZED-F9P
Cost	300,000 USD	45,000 USD	1,000-1,200 USD

3.2 Environmental Description

In order to evaluate the performance of the testing system and assess the advancements offered by RIMU, the experiment is conducted in three distinct environments representing diverse scenarios. These environments include an open sky scenario (highway), a GNSS challenging scenario (narrow alley), and a GNSS outage scenario (underground parking garage). The selection of these environments aims to provide a comprehensive analysis of the system's behavior and the potential benefits introduced by RIMU technology.

The open sky scenario is primarily conducted on a highway located in Tainan, Taiwan, involving the vehicle being driven at a high speed of approximately 100 km/hr. The initial alignment phase, which comprises static, straight ahead, and multiple turning, is performed in an open area. To ensure accurate analysis, the period of initial alignment is excluded from the data set. The duration of the included travel time for this open sky scenario amounts to approximately 15 minutes.

The GNSS challenging scenario takes place within a residential area situated in the Tainan City center, Taiwan. In this scenario, the presence of narrow alleys introduces challenges such as Multipath Interference and Non-line-of-sight Reception. These factors can potentially degrade the GNSS signal quality. The total duration of travel in this particular area amounts to approximately 20 minutes.

The GNSS outage scenario is carried out within the underground parking garage of National Cheng Kung University (NCKU) in Tainan, Taiwan. The test trajectory encompasses both outdoor and indoor environments, involving traversals of different levels, including upstairs, downstairs, and multiple turning routes. In this scenario, the analysis focuses solely on the period of GNSS outage, which lasts for approximately 5 minutes.

4. RESULTS AND DISCUSSION

This section presents the experimental results of the proposed algorithm obtained from the three scenarios. The results of using either SIMU or RIIMU within the INS/GNSS integration scheme. Additionally, the best pose derived from PwrPak7D-E2 is seen as the benchmark, which represents the output of the position obtained from the integrated INS/GNSS solution embedded within the system. Throughout the subsequent analyses, the reliable reference system, as previously mentioned, is employed to evaluate the two testing systems and one benchmark, ensuring accurate and reliable comparisons.

4.1 Open Sky Scenario

Figure 6 shows the experimental trajectory of the open sky scenario, and Table 4 displays the analysis of position error, which is estimated by the reference trajectory. By employing the RTK service, both the testing system and the benchmark system achieve a submeter level of accuracy. To take a close look, the utilization of RIMU yields results comparable to the benchmark, exhibiting a root mean square error (RMSE) of 0.275 meters in the horizontal direction and 0.299 meters in three-dimensional (3D) space, which can meet the requirement of "Where in Lane" (0.5 meters) level.

In this scenario, the GNSS solution exhibits high quality, leading to the accurate performance of the INS/GNSS integrated system. It is evident from the detail of the fusion trajectory and the GNSS solution that the system heavily relies on GNSS information. (Figure 7) However, a considerable enhancement of approximately 50% is still observable with the implementation of RIMU, compared to SIMU. The RIMU system not only reduces the overall error but also minimizes the maximum error, which can be even smaller than the benchmark. Consequently, the RIMU system demonstrates a higher level of availability, even in comparison to the benchmark system.

Figure 6. The trajectory of the experimental result in the open sky scenario

Figure 7. The trajectory of the zoom in experimental result in the open sky scenario

Table 4. The position analysis of experimental results in the GNSS open sky scenario

912 seconds	Benchmark					RING-RTK (RIMU)					SING-RTK (SIMU)				
Position Error (Meter)	E	N	U	2D	3D	E	N	U	2D	3D	E	N	U	2D	3D
Mean	-0.015	0.010	0.116	0.050	0.148	0.022	0.084	0.097	0.244	0.273	-0.304	-0.184	0.088	0.518	0.543
Max	-2.778	1.061	-0.538	2.871	2.871	0.661	-1.562	0.602	1.585	1.599	-1.606	-2.245	-1.547	2.253	2.434
STD	0.208	0.111	0.041	0.231	0.221	0.163	0.204	0.066	0.126	0.121	0.257	0.366	0.154	0.240	0.250
RMSE	0.208	0.112	0.123	0.236	0.267	0.164	0.221	0.118	0.275	0.299	0.398	0.409	0.178	0.571	0.598

4.2 GNSS Challenging Scenario

The experimental trajectory of the GNSS challenging scenario is displayed in Figure 8, while the corresponding analysis of position error is presented in Table 5. Notably, both the SIMU and RIMU testing systems exhibit poorer performance compared to the benchmark system. Interestingly, there is little discernible difference between the SIMU and RIMU systems, as they exhibit similar RMSE of approximately 2.3 meters in the horizontal direction and 5 meters in 3D space. Notably, the errors in the Up direction are particularly pronounced, reaching around 4.4 meters.

These outcomes can be attributed to the poor quality of the GNSS solution, as evident in the magenta rectangular area depicted in Figure 8. The usage of a low-cost GNSS receiver in the testing systems results in a comparatively poorer GNSS solution quality in challenging areas in comparison with the GNSS solution employed by the benchmark system. It is worth mentioning that the GNSS solutions exhibit system errors, likely stemming from factors such as Multipath Interference or Non-line-of-sight Reception, as these contribute to deviations from the reference trajectory.

Of particular significance, the INS/GNSS integrated system exhibits a notable dependency on the GNSS solutions within this scenario. This reliance causes the fusion solution to be continuously influenced by the GNSS solution. This hypothesis can be substantiated by examining the standard deviation (STD) and the GNSS measurement solution displayed in Figure 9. During the period highlighted by the red rectangular region, the height error can exceed 25 meters. However, the corresponding STD fails to accurately reflect the true quality of the GNSS solution. Consequently, the Extended Kalman Filter (EKF) places excessive trust in the GNSS update, ultimately leading to suboptimal outcomes. This issue might be addressed by adjusting the mode of the GNSS module, adding more fault detection into the algorithm, fine-tuning the parameters, or adopting another independent measurement such as VINS.

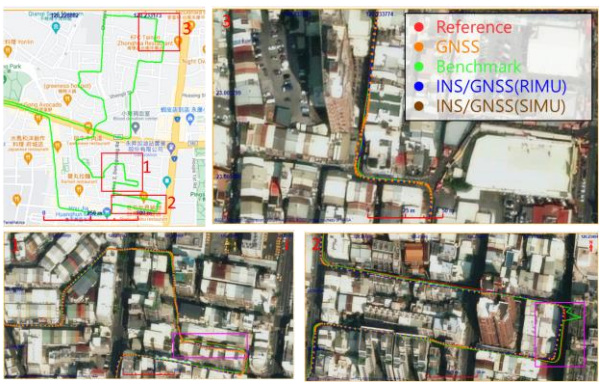

Figure 8. The trajectory of the experimental result in the GNSS challenging scenario

Table 5. The position analysis of experimental results in the GNSS challenging scenario

1297 seconds	Benchmark					RING-RTK (RIMU)					SING-RTK (SIMU)				
Position Error (Meter)	E	N	U	2D	3D	E	N	U	2D	3D	E	N	U	2D	3D
Mean	0.023	-0.048	1.317	0.893	1.606	-0.957	-0.226	2.778	1.432	3.697	-0.953	-0.222	2.355	1.491	3.491
Max	15.528	-2.373	30.323	15.529	34.068	-11.089	-4.461	13.432	11.772	13.444	-10.793	-4.359	13.128	11.354	13.159
STD	0.821	0.628	1.003	0.521	1.109	1.906	0.864	3.459	1.815	3.371	1.964	0.898	3.454	1.842	3.303
RMSE	0.821	0.629	1.656	1.035	1.953	2.133	0.893	4.437	2.312	5.003	2.183	0.925	4.181	2.370	4.806

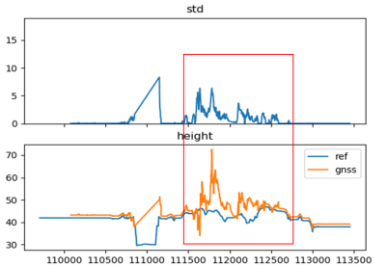

Figure 9. The standard deviation and the solution of GNSS height of the experimental result in the GNSS challenging scenario

4.3 GNSS Outage Scenario

Figure 10 displays the experimental trajectory in a long GNSS outage scenario, entering and exiting an underground parking. The trajectory encompasses a continuous downhill slope with two right-angle turns, following a reverse E-shaped path that includes multiple bends and two instances of backing up. Throughout the test, the GNSS outage duration reached approximately 5 minutes, and a detailed accuracy analysis is presented in Table 6. Comparing the performance of the benchmark system with testing systems using SIMU and RIMU, it is evident that the algorithm employed in the test system demonstrates superior functionality compared to the benchmark system. To take a close look, the RIMU system shows an RMSE of 3.255 meters in the horizontal direction and 3.302 meters in 3D space. The benchmark system, when deprived of GNSS updates, experiences system failure and substantial positioning errors arising from the long-term accumulation of IMU errors.

Moreover, RIMU exhibits a noteworthy improvement in position accuracy (about 60%), surpassing SIMU in both the horizontal and vertical dimensions. RIMU demonstrates trajectory shapes and positions that closely resemble the reference trajectory.

This significant improvement can be attributed to the enhanced accuracy in orientation estimation, particularly pertaining to the roll and pitch angles. The presence of gravity projection in the lateral and longitudinal directions can result in considerable errors in velocity and position, particularly in scenarios involving downhill and uphill gradients. By achieving a more precise estimation of orientation, the detrimental effects of gravity projection are effectively mitigated, leading to improved overall navigation solutions.

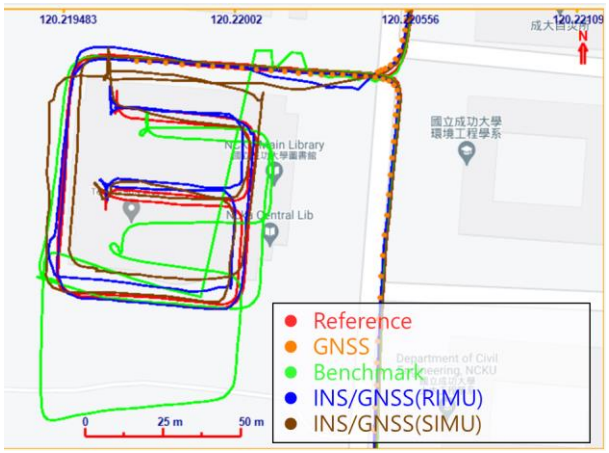

Figure 10. The trajectory of the experimental result in the GNSS outage scenario

Table 6. The position analysis of experimental results in the GNSS outage scenario

298 seconds	Benchmark					RING-RTK (RIMU)					SING-RTK (SIMU)				
Position Error (Meter)	E	N	U	2D	3D	E	N	U	2D	3D	E	N	U	2D	3D
Mean	1.789	-13.544	2.594	17.175	17.436	-0.981	1.674	0.202	2.821	2.888	-1.685	4.406	-1.510	7.311	7.596
Max	-15.985	-72.996	10.488	73.603	74.346	-5.584	6.044	2.283	6.949	6.949	-25.417	17.723	-3.861	25.570	25.859
STD	6.374	18.961	2.770	17.072	17.229	1.339	2.244	0.518	**1.622**	**1.600**	4.890	5.429	0.684	4.709	4.548
RMSE	6.621	23.315	3.798	24.237	24.533	1.660	2.799	0.556	**3.255**	**3.302**	5.173	6.992	1.658	8.698	8.854

5. CONCLUSION

Figure 11, Figure 12, and Figure 13 illustrate the cumulative distribution function (CDF) of the 3D position error. Examining the 68% confidence level, it is observed that the testing system utilizing RIMU maintains position errors below 5 meters across all three scenarios. In contrast, the SIMU system exhibits errors reaching up to 10 meters, while the benchmark system experiences errors of up to 15 meters. These findings underscore the superior accuracy and availability of RIMU, particularly in GNSS outage scenarios.

In the open sky scenario, the RIMU system exhibits significant improvement compared to the SIMU system. Meanwhile, the benchmark system consistently demonstrates smaller errors than the RIMU system throughout most of the observation period. However, the cumulative distribution function (CDF) curve for the RIMU system approaches 100% with smaller errors, indicating the occurrence of infrequent but significant errors that the benchmark system struggles to address (as evidenced by the previously mentioned maximum error in Table 4). Consequently, these factors contribute to the small difference in RMSE between the two systems. In essence, the testing RIMU system offers enhanced availability, proving capable of handling exceptional situations with improved performance.

In the context of GNSS challenging scenarios, the benchmark system outperforms the two testing systems due to disparities in

the GNSS solutions employed. The benchmark system, equipped with a higher-cost GNSS receiver boasting superior specifications, exhibits better performance. To address this issue, one potential solution is to integrate an independent low-cost navigation system, such as Visual-Inertial Navigation System (VINS), to detect and compensate for faults in the GNSS solutions. By leveraging VINS technology, it becomes possible to identify erroneous GNSS measurements and enhance the overall robustness of the system.

Overall, the integration of a low-cost RIMU, GNSS receiver, and proposed integrated algorithm yields a system that achieves a balance between accuracy and availability, resulting in enhanced environmental adaptability. The comprehensive evaluation of this system highlights its potential for the development of a Robust Autonomous Vehicular Navigation System.

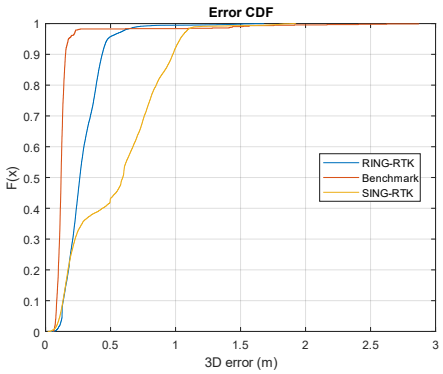

Figure 11. The cumulative distribution function of 3D position error in the open sky scenario

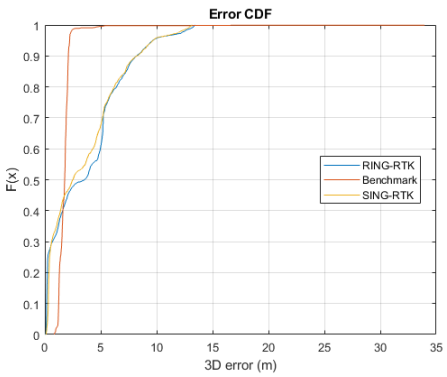

Figure 12. The cumulative distribution function of 3D position error in the GNSS challenging scenario

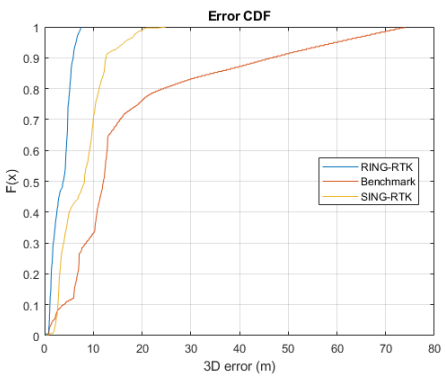

Figure 13. The cumulative distribution function of 3D position error in the GNSS outage scenario

ACKNOWLEDGEMENTS

The authors would like to thank The National Science and Technology Council (NSTC), ROC (Taiwan) for providing financial support. Additionally, the AI tool, ChatGPT developed by OpenAI was used to polish part of manuscript.

REFERENCES

SAE International, “Taxonomy and Definitions for Terms Related to Driving Automation Systems for On-Road Motor Vehicles (J3016B),” Tech. Rep., 2018.

Reid, T.G.R., Houts, S.E., Cammarata, R., Mills, G., Agarwal, S., Vora, A., and Pandey, G. (2019) Localization Requirements for Autonomous Vehicles. In Proceedings of the WCX SAE World Congress Experience 2019, Detroit, MI, USA.

Alves, P., Williams, T., Basnayake, C., & Lachapelle, G. (2010). Can GNSS Drive V2X. GPS World, 21(10), 35-43.

Stephenson, S. (2016). Automotive applications of high precision GNSS, Doctoral dissertation, University of Nottingham.

N. El-Sheimy, “Inertial Techniques and INS/DGPS Integration,” ENGO 623-Course Notes, University of Calgary, Calgary, 2006.

A. Waegli, S. Guerrier and J. Skaloud, "Redundant MEMS-IMU integrated with GPS for performance assessment in sports," 2008 IEEE/ION Position, Location and Navigation Symposium, Monterey, CA, USA, 2008, pp. 1260-1268, doi: 10.1109/PLANS.2008.4570079.

Jafari, M. (2015). Optimal redundant sensor configuration for accuracy increasing in space inertial navigation system. Aerospace Science and Technology, 47, 467-472.

Martin, H., Groves, P. D., Newman, M., & Faragher, R. (2013, September). A new approach to better low-cost MEMS IMU performance using sensor arrays. In Proceedings of the 26th International Technical Meeting of the Satellite Division of The Institute of Navigation (ION GNSS+ 2013) (pp. 2125-2142).

Y. H. Cho, W. J. Park and C. G. Park, "Novel Methods of Mitigating Lever Arm Effect in Redundant IMU," in IEEE Sensors Journal, vol. 21, no. 7, pp. 9465-9474, 1 April1, 2021, doi: 10.1109/JSEN.2021.3054945.

Bancroft JB, Lachapelle G. Data fusion algorithms for multiple inertial measurement units. Sensors (Basel). 2011;11(7):6771-98. doi: 10.3390/s110706771. Epub 2011 Jun 29. PMID: 22163985; PMCID: PMC3231672.

N. El-Sheimy, H. Hou and X. Niu, "Analysis and Modeling of Inertial Sensors Using Allan Variance," in IEEE Transactions on Instrumentation and Measurement, vol. 57, no. 1, pp. 140-149, Jan. 2008, doi: 10.1109/TIM.2007.908635.

de Alteriis G, Accardo D, Conte C, Schiano Lo Moriello R. Performance Enhancement of Consumer-Grade MEMS Sensors through Geometrical Redundancy. Sensors (Basel). 2021 Jul 16;21(14):4851. doi: 10.3390/s21144851. PMID: 34300592; PMCID: PMC8309765.